Original Article

Field and Numerical Assessment of Geogrid-Reinforced **Embankments Over Soft Clay**

Ali Gamal Abdel Zaher^{1*}, Samir Abdelfattah¹, Mostafa Merzk¹, Sherif Abdelaziz Mazk²

¹Department of Civil Engineering, Al-Azhar University, Cairo, Egypt. ²Department of Civil Engineering, Military Technical College, Cairo, Egypt.

*Corresponding Author: aliabdelmoneim.1425@azhar.edu.eg

Received: 10 September 2025 Revised: 11 October 2025 Accepted: 09 November 2025 Published: 29 November 2025

Abstract - Soft clay deposits in Egypt's northern Nile Delta create persistent problems for canal and embankment construction. The soil at the site is soft and highly compressible, with limited drainage, which often leads to large settlements and instability of the slope. In this work, a geogrid-reinforced embankment was used as a simple and economical method to improve the behavior of slopes resting on soft clay. The embankment was constructed from compacted sand layers separated by biaxial geogrids and supported on a crushed-stone layer about one meter thick. This foundation rested on roughly ten meters of soft clay. Field monitoring using settlement plates and inclinometers was carried out to record the vertical and horizontal ground movements during service conditions. A 2D numerical model was created in PLAXIS 2D and then modified according to the field measurements. The results from the model were very similar to the real recorded data, which means that the model could simulate the actual soil and structure behavior with good accuracy. After confirming this consistency, additional analyses were carried out to explore how variations in soil properties and reinforcement characteristics could influence the overall response of the system. The results indicated that higher geogrid stiffness and smaller vertical spacing improved slope stability, while a thicker stone base helped reduce settlement. The findings provide practical direction for engineers to design safer and more economical reinforced embankments under similar ground conditions.

Keywords - Embankment stability, Finite element modeling, Geogrid reinforcements, Soft clays, Soil improvements.

1. Introduction

Constructing embankments on soft clay is one of the most difficult geotechnical problems faced in the Nile Delta region. The soil in these areas is very weak in shear, highly compressible, and drains water slowly. Because of these characteristics, the soil often cannot carry construction loads safely, leading to large settlements, lateral movement, and loss of slope stability [1, 2]. To deal with such poor conditions, several ground improvement methods have been used. Common examples include Prefabricated Vertical Drains (PVD), vacuum preloading, and combinations of drains with rigid inclusions such as cement or chemical grouting. Other techniques use column-like supports, including piled embankments, stone columns, and soil mixing columns (DSM) [3].

In recent years, geosynthetic materials have become more popular in soft soil improvement because they are economical, easy to install, and adaptable to many ground conditions. Among them, geogrids have shown good performance in strengthening embankments, retaining walls, and shallow foundations. Geogrids are lightweight and resistant to corrosion, and they can withstand large strains without losing strength [4]. Compared with geotextiles, geogrids have an open net-like structure that interlocks with surrounding granular soil, improving load transfer and stability [5].

Experimental and numerical studies have confirmed that geogrid layers improve stress distribution and reduce differential settlement in soft subgrades[6]. This improvement mainly comes from three actions: friction along the geogrid ribs, passive resistance on the transverse members, and the interlocking of soil grains inside the openings. Finite element modelling has shown that these actions are more effective when the geogrid is embedded in compacted sand layers placed above soft clay [7].

For the design of reinforced soil systems, two main conditions must be satisfied: the reinforcement should not fail by tension or deformation, and it should have enough length to prevent pull-out from the soil. These factors control the choice of geogrid strength, spacing, and embedment depth. Optimizing these parameters improves the bearing capacity and overall safety of the structure. Many studies have examined the performance of reinforced soil through laboratory and numerical investigations. Results indicate that the number and spacing of reinforcement layers, as well as the type of geogrid, have a strong influence on the settlement of reinforced foundations [8].

Numerical simulations using PLAXIS 2D also proved that higher tensile stiffness in the geogrid increases the factor of safety and reduces deformation [9]. Other researchers studied reinforced slopes under seismic or nonuniform loading and found that reinforcement is most effective near the middepth zones [10].

Further research highlighted that combining geogrids with a stiff granular platform, such as compacted crushed stone, can significantly enhance the overall response of embankments [11-13]. This composite system provides better load distribution, minimizes settlement, and limits lateral displacement.

This study presents a real case from a canal embankment located in the northern Nile Delta region in Egypt. The embankment was built over a weak clay layer and supported with a combined improvement system that included a crushed stone working platform together with alternating layers of sand and geogrid. During operation, settlement plates and inclinometers were installed to track the vertical settlement and lateral ground movement.

In order to understand how the ground actually behaved on site, I built a simple two-dimensional model in PLAXIS 2D. The geometry and loading used in the model followed what was present in the canal area, including the lining. After running the first trial, the results were compared with the field records, and then some adjustments were made to get closer to the real measurements. Eventually, the model results showed almost the same trend as the field data, which gave reasonable confidence in the model.

In the following stage of the study, I carried out a parametric analysis to see how changes in soil conditions and reinforcement details could affect the behavior of the embankment. Different factors were considered, including the stiffness and spacing of the geogrid layers, the thickness of the crushed stone layer, and some of the clay properties such as cohesion, elastic modulus, unit weight, and the thickness of the soft layer. Based on the analysis, it was noticeable that each parameter had a clear impact on the embankment performance.

For example, reducing the spacing between the geogrid layers and using stiffer reinforcement led to better slope stability and smaller ground movements in both directions. Also, when the clay had better mechanical properties, the amount of settlement decreased and the safety increased. These outcomes help in choosing the suitable number of geogrid layers and the suitable thickness of the granular layer so that the design remains safe and at the same time avoids unnecessary cost for embankments built on soft clay.

2. Materials and Methods

2.1. Site Description

The canal cross-section is located in Hammam town, Alexandria, Egypt, as shown in Figure 1. The study is carried out on a canal-side slope embankment comprising layers of geogrids alternating with sand and a crushed stone foundation layer beneath for the El-Hamam Canal Construction, based on soil investigation work from St 35+000 to St 40+935.

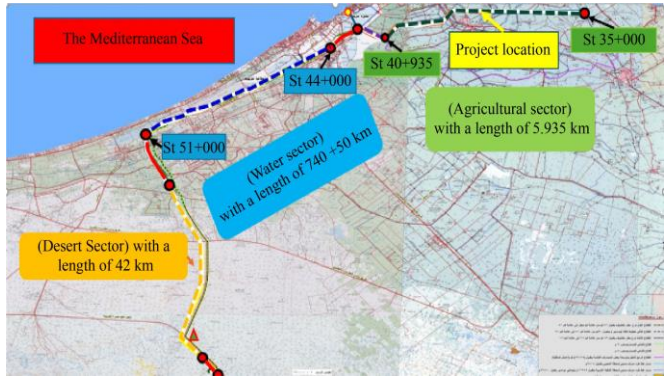


Fig. 1 Location map of the El-Hamam Canal project showing the agricultural, water, and desert sectors in the northern Nile Delta, Egypt

2.2. Embankment Geometry and Reinforcement Layout

The embankment was constructed with eleven alternating layers of compacted sand and biaxial geogrid reinforcement. The geogrid layers were installed at a constant vertical spacing of 0.30 m, forming a side slope inclined at 3H:1V. A 1.0 m-thick layer of well-compacted crushed stone was placed at the foundation level to improve the overall bearing capacity of the soft clay and to minimize long-term settlement.

Subsurface exploration carried out through boreholes and laboratory testing confirmed the presence of a soft clay stratum about 10 m thick directly beneath the embankment, underlain by a dense sand layer extending approximately 25 m. The physical and mechanical properties of these soils were determined and classified according to the Egyptian Code of Soil Mechanics. The geometry and reinforcement configuration of the embankment are shown in Figure 2.

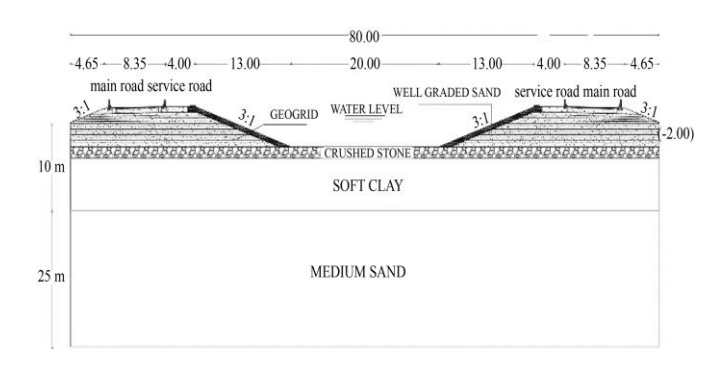


Fig. 2 Cross-section of the geogrid-reinforced road embankment illustrating the arrangement of the sand layers, geogrid sheets, and the crushed stone foundation over soft clay

2.3. Geogrid Reinforcement System

Biaxial geogrids were used as reinforcement in this project because they provide tensile stiffness in both the longitudinal and transverse directions [14]. This dual strength helps confine the soil laterally, limits differential settlement, and ensures better load distribution within the embankment. The main physical and mechanical properties of the geogrid, as specified by the manufacturer, are summarized in Table 1.

Table 1. Tensile stiffness properties of the geogrid

Table 1: Tensite surfices properties of the geogra		
Parameters	Values	
Structure	Biaxial	
Aperture shape	Squared	
Aperture size	37 mm×37mm	
Mass per unit area	360 g/m2	
UV resistance	>94 %	
Raw material	Polypropylene	
Elongation at nominal strength	11 %	
Tensile strength (Tult)	30(KN/m)	
Tensile stiffness (EA)	300(KN/m)	

2.4. Field Execution of the Geogrid - Reinforced Embankment

The geogrid-reinforced canal embankment was built through a sequence of controlled construction steps to ensure soil stability and proper load transfer. Work started with excavation down to the design bed level at an elevation of -5.165 m, which is about 3.165 m below the existing ground surface (-2.00 m).

- a) A 1.0-meter-thick crushed stone replacement layer was placed and compacted in four successive lifts, each about 25 cm thick, using a 27-ton dynamic roller. This layer of crushed stone had multiple functions. First, it helped distribute the load over the ground so the soft clay below did not receive high stresses, and it provided a firm base for the next construction works. It also improved drainage because the water pressure could dissipate more easily during loading. A plate-load test on the layer indicated an allowable bearing capacity of around 225 kPa, which falls within the range stated in the Egyptian Code.
- b) After compacting the crushed-stone layer, biaxial geogrid layers were placed directly above it. Their alignment and spacing were checked carefully to make sure they worked in both directions.
- c) After placing each geogrid layer, a layer of clean sand was spread on top and compacted to roughly 95% of its maximum dry density. This helped the sand make good contact with the geogrid, improving load distribution and the overall stability of the embankment [15]. Since the sand was well-graded, it also allowed water to drain easily, reducing pore water pressure in the upper fill. The side slopes were then covered with about 40 cm of crushed stone over a 400-micron geotextile sheet for protection.

d) Concrete blocks were placed on top of the embankment to simulate the effects of canal water and nearby structures. This acted as a preload to speed up the consolidation of the soft clay and allowed us to observe the embankment's response early. Figure 3 shows the construction process.









Fig. 3 Shows the steps followed during the field construction of the reinforced canal embankment: (a) Placing the crushed stone, (b) Installing the geogrid, (c) Adding the sand fill, and (d) The completed embankment with the concrete blocks in place.

2.5. Field Monitoring and Experimental Methodology

We placed monitoring instruments on each side of the canal to see how the embankment behaved under the simulated service conditions. The system was designed to record field behaviour during loading and included several instruments placed at critical locations:

- Vertical displacement monitoring devices.
- Inclinometers for measuring lateral movements.
- Strain gauges to monitor the behaviour of geogrid layers.

A total of 21 (P1–P21) were installed above the crushed stone layer at the canal bed to monitor vertical displacements, as illustrated in Figure 4. The locations of the field monitoring points used in this study are illustrated in Figure 5.

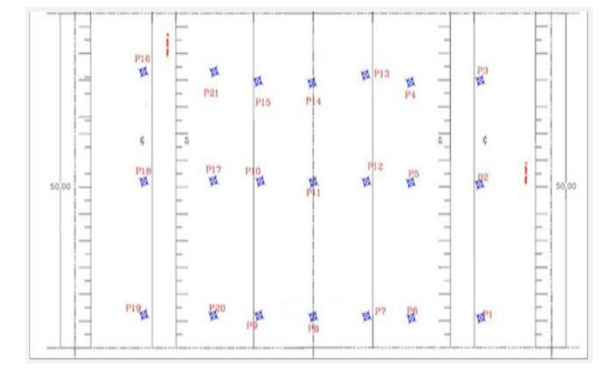


Fig. 4 Plan view illustrating the arrangement of monitoring points used to record vertical ground surface displacements at the site



Fig. 5 Field locations of vertical displacement monitoring points at the site

Two inclinometers were used to measure horizontal movement at the site. The first was placed within the embankment, and the second was fixed close to the canal slope, as illustrated in Figure 6.

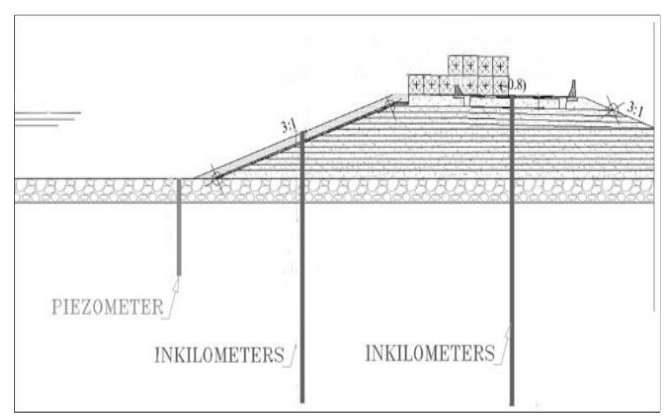


Fig. 6 Location of the inclinometer used to measure horizontal displacement within the site

A piezometer beneath the canal bed recorded changes in groundwater level throughout the loading test. The placement of the inclinometers is illustrated in Figure 7.



Fig. 7 The position of the inclinometer used for horizontal displacement monitoring

2.6. Numerical Model

PLAXIS 2D software version V21 was utilized to perform finite element analysis and simulate the soil–structure interaction under realistic field conditions. The model accounted for complex stress redistribution within the embankment and foundation soils due to construction activities and the presence of water inside the concrete canal. A detailed simulation was carried out to capture both vertical and lateral deformations, pore pressure variations, and load transfer mechanisms.

Using a two-dimensional model was considered suitable for this work because the canal embankment has almost the same shape and loading conditions along its length. The way the structure behaved mostly depended on its cross-section, which was designed to meet the plane strain requirement. This made it easier to look at how the soil and reinforcement worked together, especially in the areas where displacements were largest.

Field data were used to adjust the model so it matched the observed soil and embankment behavior. Sensitivity checks showed that a $180 \text{ m} \times 80 \text{ m}$ domain kept boundary effects small. A finer mesh near the embankment helped get more accurate stress and displacement results, see Figure 8.

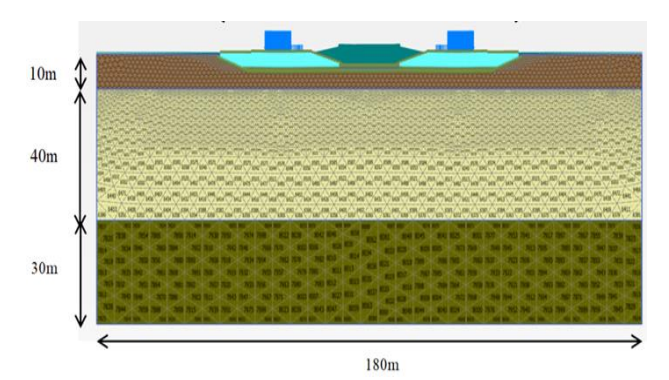


Fig. 8 Shows the finite element model with its boundary conditions and mesh arrangement

2.7. Soil Parameters and Material Properties

The soil layers in the numerical model were set according to what we found from field and lab tests, including the Standard Penetration Test(SPT), grain size analysis, Atterberg limit determination, and both unconfined compression and triaxial shear tests.

Based on the collected data, three distinct soil layers were identified: a very soft clay deposit, a compacted embankment sand layer, and a sub-base sand layer. The Hardening Soil Model (HSM) was selected for all layers, as it provides a better description of stress-dependent stiffness and nonlinear stress-strain response under different drainage conditions. The main geotechnical parameters used in the analysis are listed in Table 2.

Table 2. Geotechnical properties of the soil layers adopted in the numerical model				
Soil Parameter	Subbase Sand	Soft clay	Embankment Sand	
Material Model	Hardening soil	Hardening soil	Hardening soil	
unit weight (kN/m³)	17	17	18	
Drainage Type	Undrain A	Undrain A	drained	
$\frac{E_{50}^{\text{ ref}}}{(kN/m^2)}$	60000	2000	60000	
$\frac{{\rm E_{\rm oed}}^{\rm ref}}{({\rm kN/m^2})}$	60000	2000	60000	
$\frac{E_{ur}^{\ ref}}{(kN/m^2)}$	180000	6000	180000	
Power (m)	1	1	1	
c (kN/m²)	1	13	1	
φ (°)	36	23	36	
ψ (°)	6	0	6	
OCR		1		

0.7

3. Result and Discussion

 R_{inter}

3.1. Model Verification

Model verification was conducted to check that the finite element analysis could reasonably reproduce the field behavior of the canal embankment in El Hammam, Alexandria. The comparison between field monitoring data and the computed results was used to confirm that the model gives realistic predictions under actual working conditions. A geogrid-reinforced embankment model was adopted to validate the modeling approach used in this study. The embankment sand, soft clay layer, underlying sand layer, and the 1-meter crushed stone foundation were modeled using the Hardening Soil Model (HSM) to simulate realistic soil behavior. As shown in Figures 9 and 10, contour lines of vertical and horizontal displacements were extracted to identify the most critical locations within the embankment.

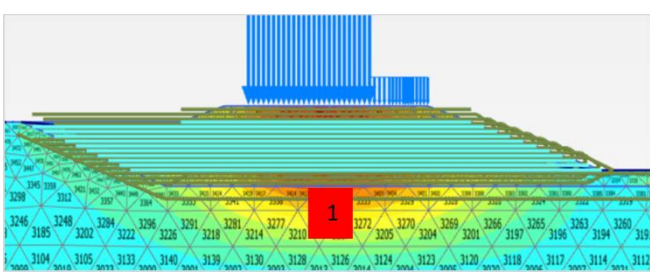


Fig. 9 Vertical displacement contour lines

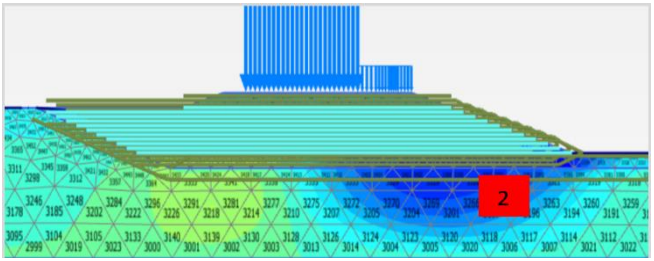


Fig. 10 Horizontal displacement contour lines

Based on these results, points 1 and 2 were selected for detailed comparison. The computed vertical displacement at Point 1 was compared with field measurements, as shown in Figure 11, while the horizontal displacement at Point 2 was evaluated in a similar manner and is presented in Figure 12. The comparison revealed a close match between the measured and simulated responses, indicating that the developed finite element model can realistically represent the long-term behaviour of the reinforced embankment under the existing conditions.

0.7

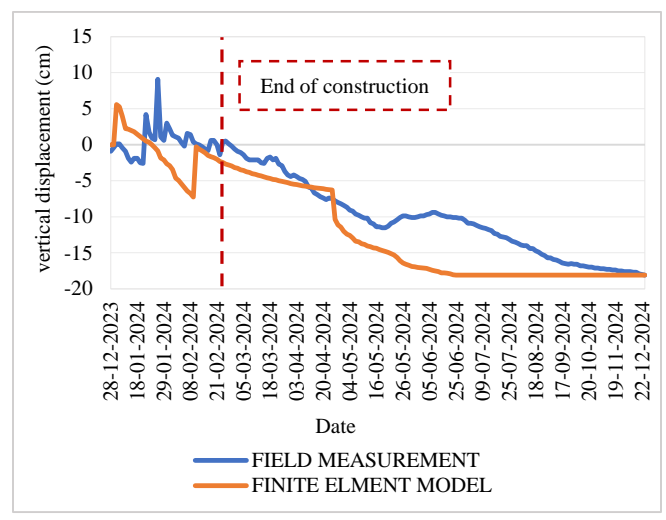


Fig. 11 Measured versus computed vertical displacement at monitoring Point 1

Figure 11 shows the verification of vertical displacement at the monitoring point. The field measurements showed a settlement of about 18.1 cm, while the finite element model gave 18.7 cm. The results were very close, around 97% accuracy, which shows that the model can reliably simulate the embankment's behavior under loading.

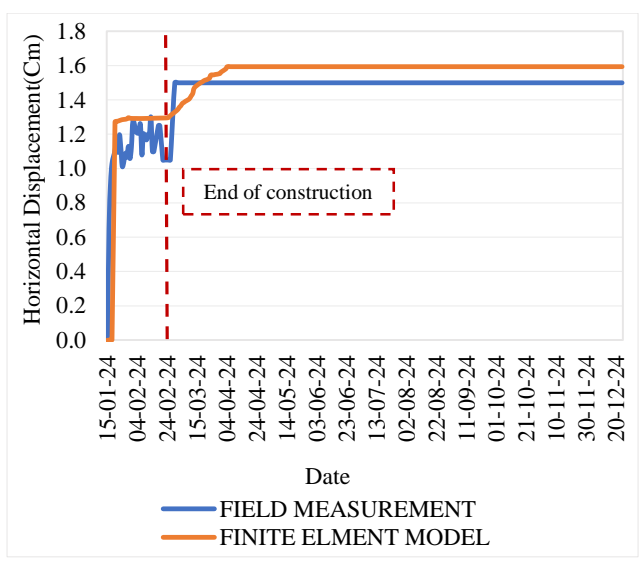


Fig. 12 Compares the measured and predicted horizontal displacement at monitoring Point 2

In Figure 12, we looked at how the monitoring point moved horizontally. In the field, it moved about 1.50 cm, and the model predicted 1.59 cm. The difference was very small, around 94%, which shows that the model does a good job of capturing how the embankment actually behaved.

3.2. Parametric Study

We ran several parametric analyses to see what affects the behavior of the geogrid-reinforced embankment on soft clay. The verified finite element model was used to test different conditions and check how changes in soil properties and reinforcement details influenced the overall performance. The results were then compared to understand their effect on both deformation and stability.

The parameters were divided into two main groups:

- Geogrid and reinforcement factors:
 - 1. Geogrid axial stiffness (EA)
 - 2. Geogrid spacing (S)
 - 3. Thickness of the crushed stone layer above the clay (T)
- Soil-related parameters:
 - 1. Cohesion of the soft clay (c)
 - 2. Modulus of elasticity of the soft clay (E)
 - 3. Unit weight of the soft clay (U)
 - 4. Thickness of the soft clay layer (D)

The ranges of values adopted in this study were selected to reflect the actual conditions of soft clay soils in the Nile Delta region, while the geogrid properties were chosen within the commonly accepted limits used in practical engineering designs. Their influence was analyzed in terms of vertical and horizontal displacements as well as the global Factor of Safety (FOS), providing valuable insights into the design optimization of the reinforced embankment system.

3.2.1. Effect of Tensile Stiffness (EA)

Figures 13 to 15 show the results of the finite element analysis of Vertical displacement, Horizontal displacement, and factor of safety with the investigated tensile stiffness of 300 KN/m, 600 KN/m, 900 KN/m, 5000 KN/m, 20000 KN/m, and 30000KN/m, under different loading conditions of 33 KN/m, 60 KN/m, 90 KN/m.

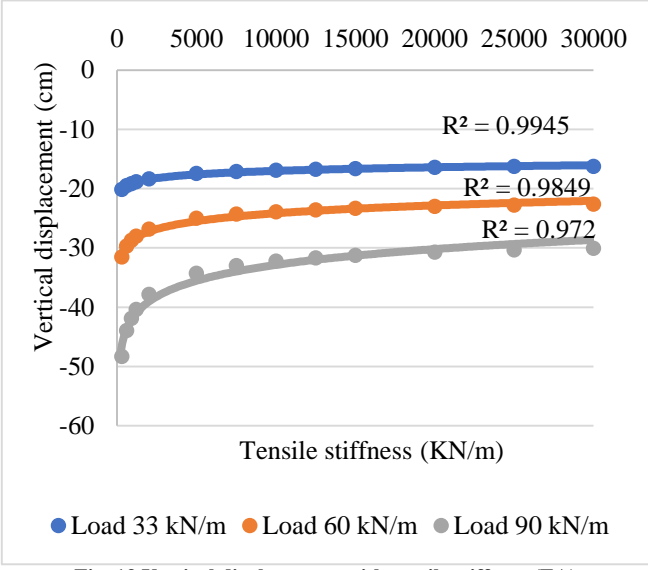


Fig. 13 Vertical displacement with tensile stiffness (EA)

Figure 13 that it can be noticed that as axial stiffness increases, vertical displacement decreases, up to a specific range depending on the applied load. For a load of 33 kN/m, vertical displacement decreases with increasing stiffness until EA reaches approximately 5000–6500 kN/m, beyond which further increases in stiffness have minimal impact. For a load of 60 kN/m, this effective range shifts to EA = 7500-10000 kN/m, while for a load of 90 kN/m, the range extends to EA = 12000-15000 kN/m. The reduction in Vertical displacement for loads of 33, 60, and 90 kN/m is 19.4%, 28.3%, and 37.9%, respectively.

Accordingly, the vertical displacement was estimated as a function of the geogrid tensile stiffness using the empirical relationships given in Equations (1) - (3):

$$VD = 0.8783 \ln(EA) - 25.09$$

(P < 0.01) load 33 kN/m (1)

$$VD = 1.9173 \ln(EA) - 41.818$$

 $(P < 0.01) \quad \text{load } 60 \text{ kN/m}$ (2)

$$VD = 3.8487 \ln(EA) - 68.318$$

(P < 0.01) load 90 kN/m (3)

Where:

VD = Vertical displacement (cm), EA= Tensile stiffness (KN/m)

The tensile stiffness of the geogrid (EA) has a clear effect on embankment performance. Choosing the right value can make the embankment more stable, reduce deformations, and may even allow using fewer reinforcement layers, which lowers construction costs for canal embankments in the North Delta.

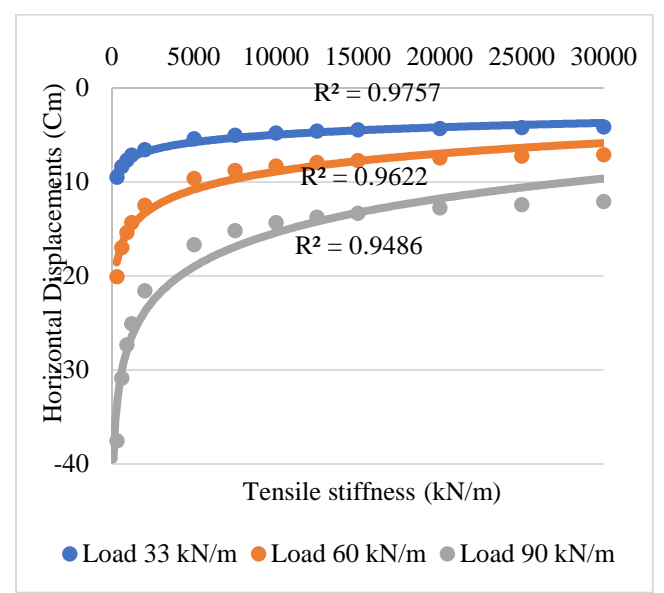


Fig. 14 Shows how horizontal displacement changes with the geogrid's tensile stiffness (EA)

Figure 14 shows that horizontal displacement gets smaller as the geogrid's axial stiffness increases. For a surface load of 33 kN/m, the displacement keeps decreasing until the stiffness reaches about 5000–6500 kN/m. Beyond that, increasing stiffness further has little effect.

When the applied load is 60 kN/m, the effective range shifts to roughly 7500–10000 kN/m, and for 90 kN/m, it extends to around 12000–15000 kN/m. The horizontal displacement decreases by 56.8%, 64.5%, and 67.8% for the same load conditions.

Accordingly, the Horizontal displacement was estimated as a function of the geogrid tensile stiffness using the empirical relationships given in Equations (4) - (6):

$$HD = 1.1485 \ln(EA) - 15.549$$

(P < 0.01) load 33 kN/m (4)

$$HD = 2.7639 \ln(EA) - 34.345$$

(P < 0.01) load 60 kN/m (5)

$$HD = 5.2417 \ln(EA) - 63.671$$

(P < 0.01) load 90 kN/m (6)

Where:

HD = Horizontal displacement (cm), EA = Tensile stiffness (KN/m)

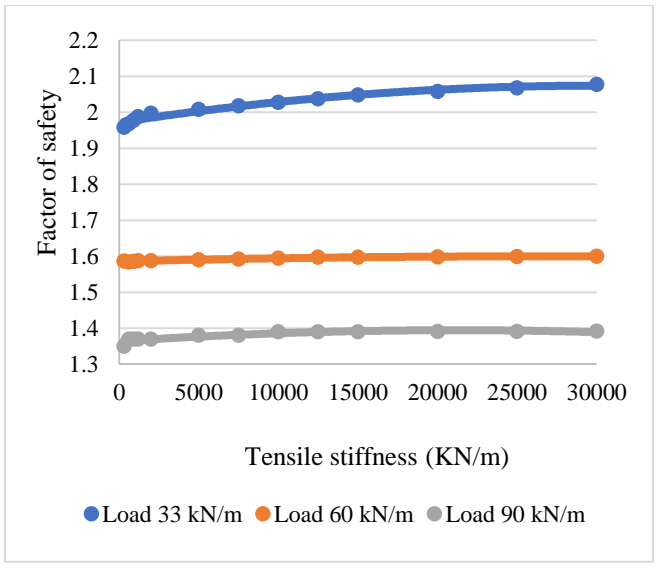


Fig. 15 The factor of safety with tensile stiffness (EA)

Figure 15 shows that the factor of safety increases with higher tensile stiffness values. As EA increases, the geogrid becomes more effective in restraining soil movement and improving load transfer, which results in a more stable slope system. This trend highlights the positive contribution of stiffer geogrid reinforcement to the global performance of the treated section.

3.2.2. Effect of Geogrid Spacing (S)

Figures 16 to 18 show the results of the finite element analysis of vertical displacement, horizontal displacement, and factor of safety with the investigation of geogrid spacing of 30 cm, 40 cm, 60 cm, 80 cm, and 120 cm, under different loading conditions of 33 KN/m, 60 KN/m, and 90 KN/m.

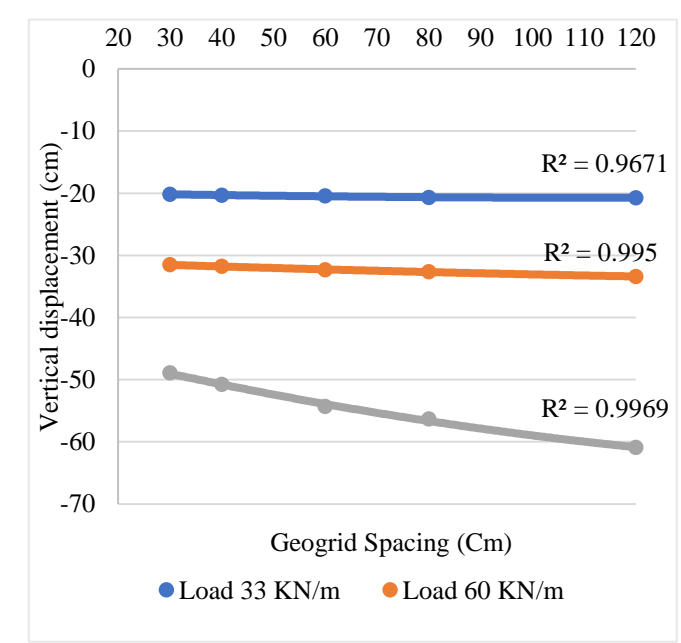


Fig. 16 Vertical displacement with geogrid spacing.

Figure 16 shows that as geogrid spacing increases, vertical displacement increases, and the variation of the geogrid spacing with the vertical displacement shows a direct relation. The increase in Vertical displacement for loads of 33, 60, and 90 kN/m is 2.9%, 6.03%, and 24.5%, respectively.

Accordingly, the Vertical displacement was estimated as a function of the geogrid spacing using the empirical relationships given in Equations (7)–(9):

$$VD = 8 \times 10^{-5} (S)^2 - 0.0177(S) - 19.718$$

(P < 0.05) load 33 kN/m (7)

$$VD = 6 \times 10^{-5} (S)^2 - 0.0295(S) - 30.702$$

(P < 0.01) load 60 kN/m (8)

$$VD = 0.0005 (S)^{2} - 0.2109 (S) - 43.174$$

$$(P < 0.05) \text{ load } 90 \text{ kN/m}$$
(9)

Where:

VD = Vertical displacement (cm), S= Geogrid Spacing (Cm)

It is important to investigate the variation in geogrid layer spacing to determine the optimal distribution that ensures the highest possible performance with the lowest cost.

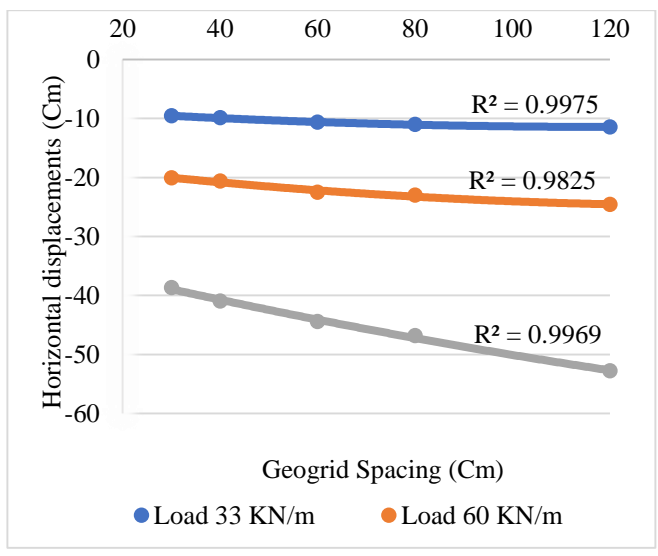


Fig. 17 Horizontal displacement with geogrid spacing

Figure 17 shows that as geogrid spacing increases, horizontal displacement increases, and the variation of the geogrid spacing with the horizontal displacement shows a direct relation. The increase in horizontal displacement for loads of 33, 60, and 90 kN/m is 19.6%, 22.5%, and 36.2%, respectively.

Accordingly, the Horizontal displacement was estimated as a function of the geogrid spacing using the empirical relationships given in Equations (10)–(12):

$$HD = 0.0002 (S)^2 - 0.0561 (S) - 8.066$$

(P < 0.05) load 33 kN/m (10)

$$HD = 0.0004 (S)^2 - 0.1034 (S) - 17.249$$

(P < 0.05) load 60 kN/m (11)

$$HD = 0.0003(S)^2 - 0.2008(S) - 33.20$$

(P < 0.01) load 90 kN/m (12)

Where:

HD = Horizontal displacement (cm), S= Geogrid Spacing (Cm)

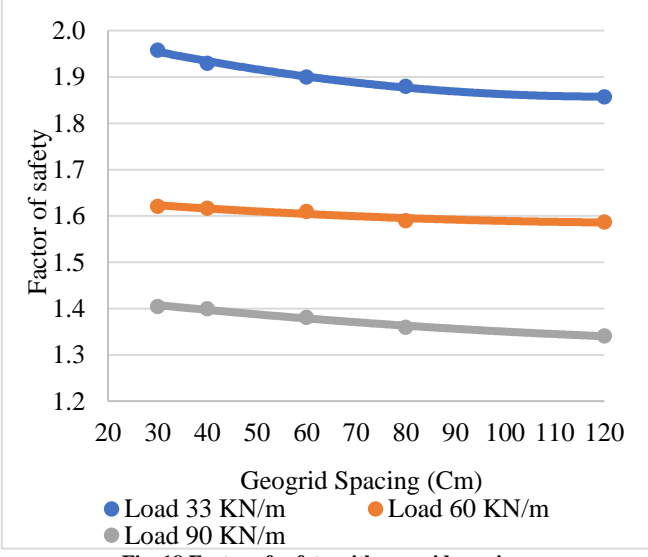


Fig. 18 Factor of safety with geogrid spacing.

Figure 18 shows an inverse relationship between geogrid spacing and the factor of safety. As the spacing between geogrid layers increases, the factor of safety decreases, indicating lower stability. This occurs because wider spacing reduces the reinforcement density and the geogrid's effectiveness in controlling soil movement.

3.2.3. Effect of Cohesion (c) for Sub-Base Soil

We conducted a series of analyses to see how the strength of the subsoil influences the behavior of a geogrid-reinforced slope. The cohesion of the soil was varied from 10 kPa to 40 kPa while applying a uniform surface load of 30 kN/m. Results showed that slopes built on stronger soil exhibited noticeably less vertical and horizontal movement.

In other words, as the soil became stiffer, it was better able to resist deformation, which improved the overall stability of the slope.

When the soil has higher cohesion, the geogrid experiences less strain because the reinforced soil mass is more stable. This also leads to a higher Factor of Safety, showing that the slope as a whole is more stable. Figures 19 to 21 illustrate these effects clearly.

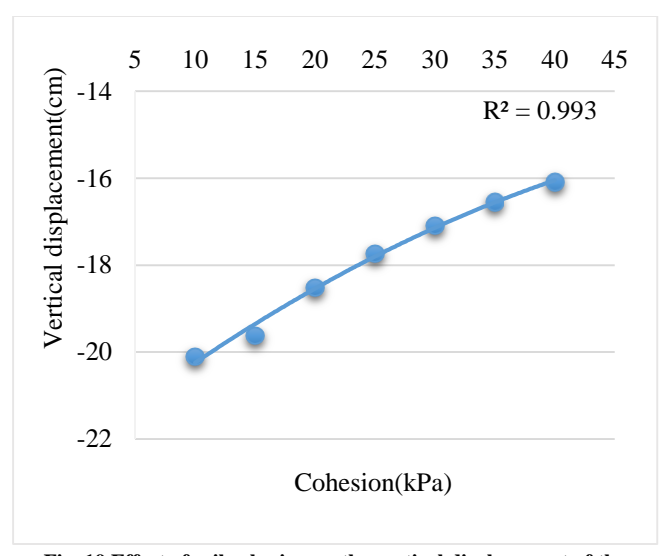


Fig. 19 Effect of soil cohesion on the vertical displacement of the embankment

Figure 19 shows that the vertical displacement gets smaller as the soil cohesion increases. When the cohesion rises from 10 kPa to 40 kPa, the settlement drops by about 19.9%. Stronger soil simply resists compression better. The horizontal displacement was then calculated from the geogrid spacing using the formula in Equation (13).

$$VD = -0.0015(C)^{2} + 0.2168(C)$$

$$- 22.6 (P < 0.001)$$
(13)

Where:

VD = Vertical displacement (cm), C= Cohesion (kPa)

The variation in cohesion can be directly utilized to guide the future design of the entire canal embankment sections across the North Delta, considering the expected changes in soil properties along the alignment

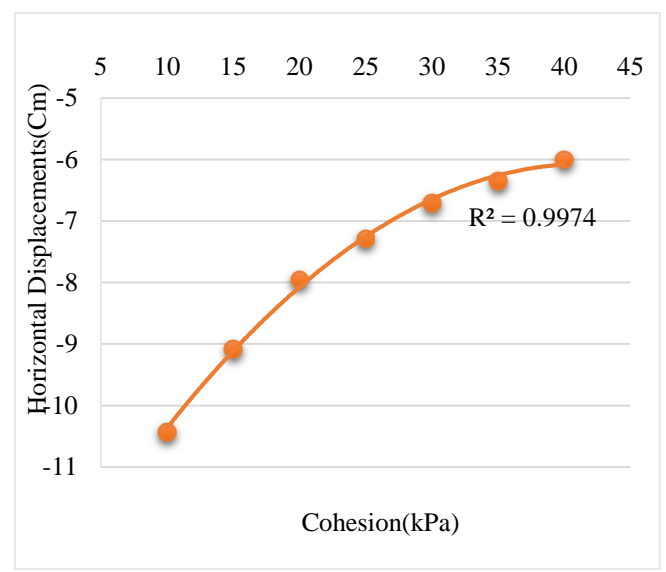


Fig. 10 Relationship between horizontal displacement and cohesion

Figure 20 illustrates that horizontal displacement tends to decrease as soil cohesion (C) increases. When the cohesion rises from 10 kPa to 40 kPa, the horizontal movement is reduced by about 42.3%

Accordingly, the Horizontal displacement was estimated as a function of the geogrid spacing using the empirical relationships given in Equation (14):

$$HD = -0.0043 (C)^{2} + 0.3582 (C) - 13.517$$

$$(P < 0.001)$$
(14)

Where:

HD = Horizontal displacement (cm), C= Cohesion (kpa)

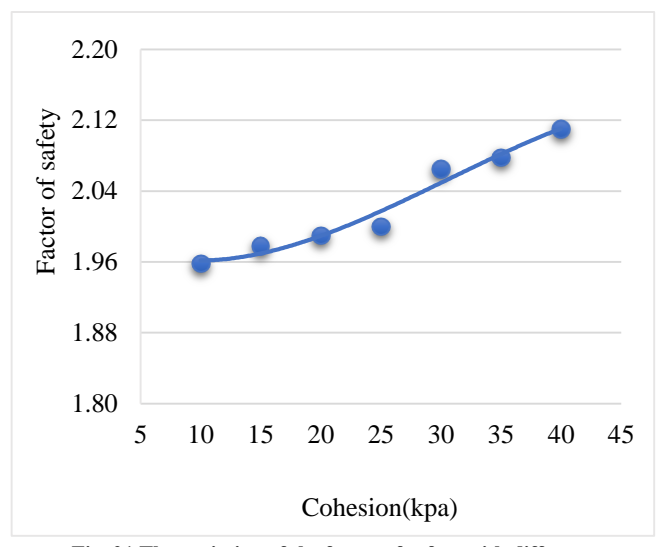


Fig. 21 The variation of the factor of safety with different cohesion values

Figure 21 indicates that the factor of safety rises as soil cohesion increases. When the clay becomes more cohesive, it can resist larger shear stresses, which limits slope movement and lowers the pressure on the geogrid layers. As a result, the entire reinforced slope performs in a more stable and balanced way under service loads.

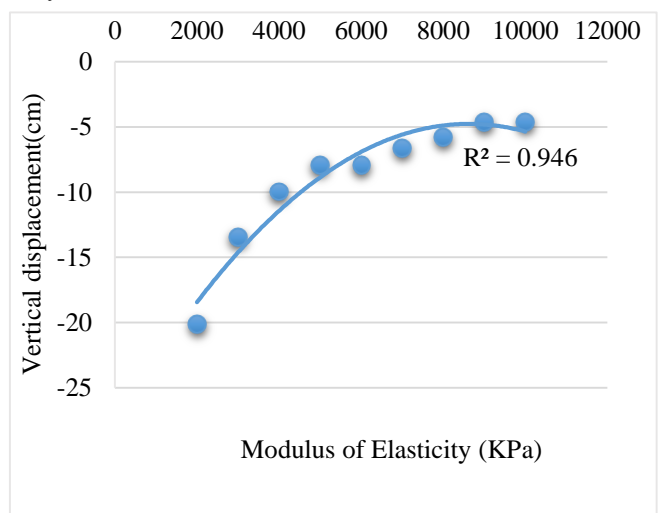


Fig. 22 Variation of vertical displacement with soil modulus of elasticity

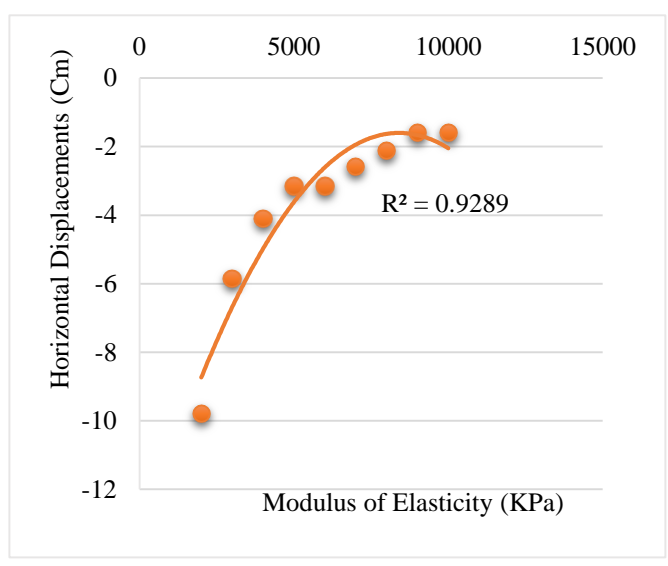


Fig. 23 Variation of horizontal displacement with soil modulus of elasticity.

3.2.4. Effect of Modulus of Elasticity (E) for Sub-Base Soil

A parametric study was carried out to examine the effect of soil stiffness on the behavior of the geogrid-reinforced slope. The soil modulus (E) ranged from 2000 to 10,000 kPa under a surface load of 30 kN/m. Results show that higher stiffness improves slope stability and reduces deformation, as presented in Figures 22 to 24.

Figure 22 illustrates that vertical displacement decreases notably with increasing modulus of elasticity, reflecting an inverse relationship between soil stiffness and settlement. When the modulus rises from 2000 kPa to 8000 kPa, the vertical deformation drops by nearly 77.1%. Beyond this range, the reduction becomes minor, indicating that further increases in stiffness have a limited effect on minimizing settlement.

Accordingly, the vertical displacement was estimated as a function of the soil modulus of elasticity using the empirical relationships given in Equation (15):

$$VD = -3 \times 10^{-7} (E)^2 + 0.0054 (E) - 27.942 (P < 0.01)$$
 (15)

Where:

VD = Vertical displacement (cm), E= Modulus of Elasticity (KPa)

Changes in the modulus of elasticity can be used as a practical guide when designing future canal embankment sections across the North Delta, since soil properties are expected to vary along the alignment.

According to Figure 23, higher stiffness leads to less horizontal displacement. The reduction is about 83.8% as the

modulus increases from 2000 to 8000 kPa. Beyond this level, the difference becomes very small, suggesting that the soil's resistance to lateral deformation doesn't improve much afterward.

Accordingly, the horizontal displacement was estimated as a function of the soil modulus of elasticity using the empirical relationships given in Equation (16):

$$HD = -2 \times 10^{-7} (E)^2 + 0.0029 (E) - 13.886$$

(P < 0.001) (16)

Where:

HD = Horizontal displacement (cm), E= Modulus of Elasticity (KPa)

3.2.5. Effect of Unit Weight (U) for Sub-Base Soil

To study how the base soil's unit weight influences the behavior of the geogrid-reinforced slope, the value was changed from 10 kN/m³ to 17 kN/m³ while keeping a surface load of 33 kN/m. The unit weight plays an important role because it controls both the self-weight of the slope and the confining stress around the reinforcement.

When the soil becomes heavier, it is more compact and better confined, which improves the bond with the geogrid and strengthens the overall response. The analysis examined vertical and horizontal displacements as well as the factor of safety. As seen in Figures 24 to 26, higher unit weight produced clear improvements in all these responses.

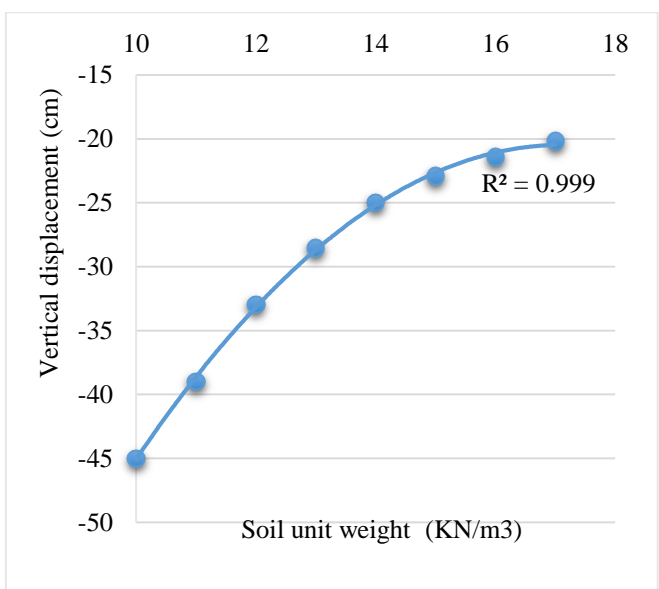


Fig. 24 Illustrates the effect of unit weight on vertical displacement

In Figure 24, we can see that the vertical displacement gets smaller as the soil unit weight goes up. When the unit weight increases from 10 to 17 kN/m³, the settlement drops by about 55%. This shows that the soil can resist compression

better because heavier soil keeps the slope more confined and stiffer. Based on this, vertical displacement was calculated as a function of soil unit weight using the empirical formula in Equation (17).

$$VD = -0.4863(U)^{2} + 16.644(U) - 162.88$$

$$(P < 0.001)$$
(17)

Where:

VD = Vertical displacement (cm), U = Unit weight (KN/m^3) .

Variations in soil unit weight can guide the design of future embankments in the North Delta, based on the different soil conditions along the route.

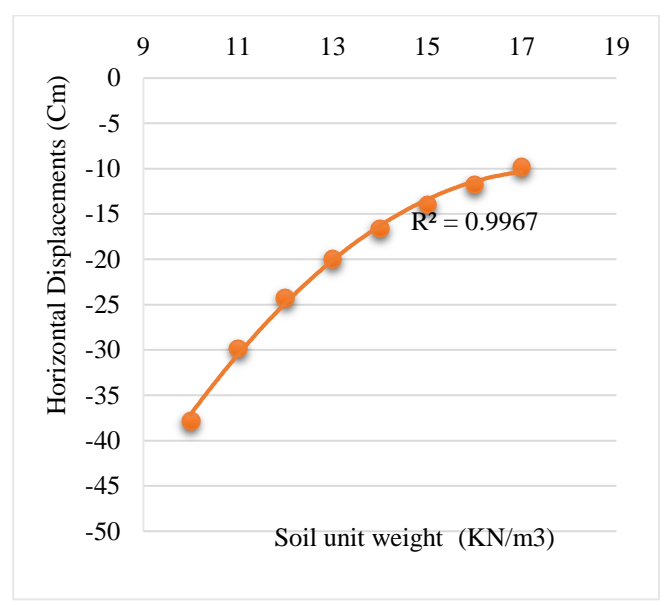


Fig. 25 Illustrates the effect of unit weight on horizontal displacement

Figure 25 shows that horizontal displacement gets much smaller as the soil unit weight increases. The slope moves less from side to side when the soil is heavier. Increasing the unit weight from 10 to $17 \, \text{kN/m}^3$ reduces horizontal movement by about 74%. Denser soil pushes back more, which helps keep the slope stable. We calculated horizontal displacement from the soil unit weight using Equation (18).

$$HD = -0.4604(U)^{2} + 16.25(U)$$

$$-153.54 (P < 0.001)$$
 (18)

Where:

HD = horizontal displacement (cm), U = Unit weight (KN/m^3) .

We looked at the slope in Figure 26. When the soil is heavier, the slope stays more stable. The extra weight pushes down on the slope. This makes the soil stronger. The strain in the geogrid becomes smaller. Heavier soil helps the slope stay steady and hold together better.

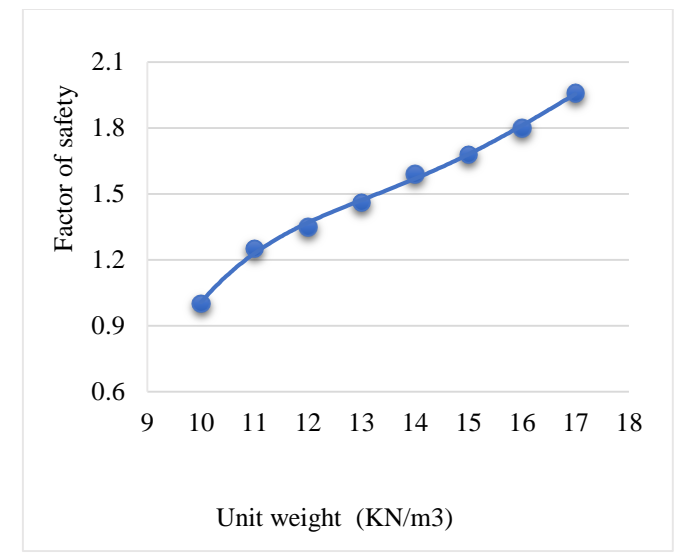


Fig. 26 Presents the slope's factor of safety for various soil unit weights

3.2.6. Impact of Sub-Base Soil Thickness (D) on Slope Behavior

We studied how the thickness of soft clay affects a geogrid-reinforced slope. We tested layers from 10 m to 20 m under a uniform surface load of 33 kN/m. Thicker clay makes the foundation more flexible, which changes how the slope moves and behaves. When the soft layer becomes thicker, both settlement and lateral movement increase, while the stability margin decreases because of the lower stiffness and strength at depth. The results were evaluated in terms of vertical and horizontal displacements as well as the factor of safety, as presented in Figures 27 to 29.

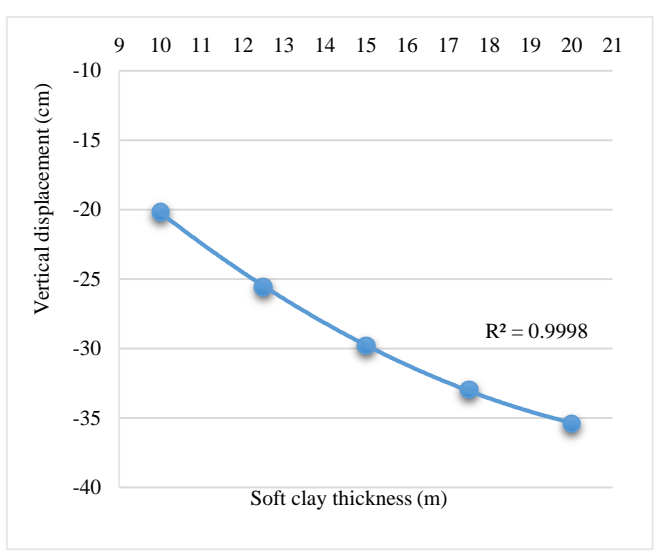


Fig. 27 Variation of vertical displacement with soft clay thickness.

Figure 27 illustrates that the vertical displacement rises notably as the soft clay layer becomes thicker. When the thickness increases from 10 m to 20 m, the total settlement grows by around 75.6%, showing that thicker clay strata are

more prone to compression and consolidation under the applied load.

Accordingly, the vertical displacement was estimated as a function of the soft clay thickness using the empirical relationships given in Equation (19):

$$VD = 0.0793(D)^{2} - 3.8938(D) + 10.8 (P < 0.001)$$
(19)

Where:

VD = Vertical displacement (cm), D = Soft clay thickness (m).

Studying the influence of soft clay layer thickness on vertical settlement offers valuable guidance for future canal embankment designs, especially since the clay thickness is expected to vary along the alignment.

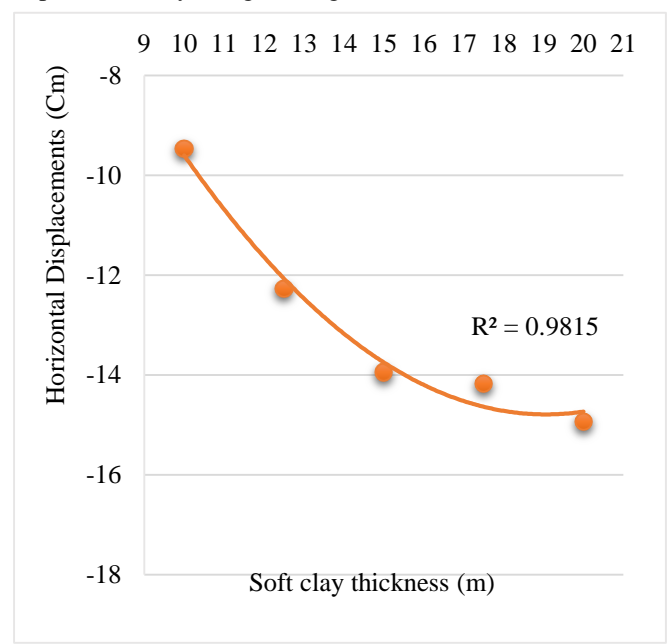


Fig. 28 Variation of horizontal displacement with soft clay thickness.

Figure 28 shows that the slope moves more sideways when the soft clay layer is thicker. Going from 10 m to 20 m of clay increases the horizontal displacement by about 57.8%. Thicker clay layers simply allow the slope to spread more, since the soil is weaker and offers less confinement.

Accordingly, the horizontal displacement was estimated as a function of the soft clay thickness using the empirical relationships given in Equation (20):

$$HD = 0.0633(D)^{2} - 2.4115(D) + 8.1918 (P < 0.001)$$
 (20)

Where:

HD = Horizontal displacement (cm), D = Soft clay thickness (m)

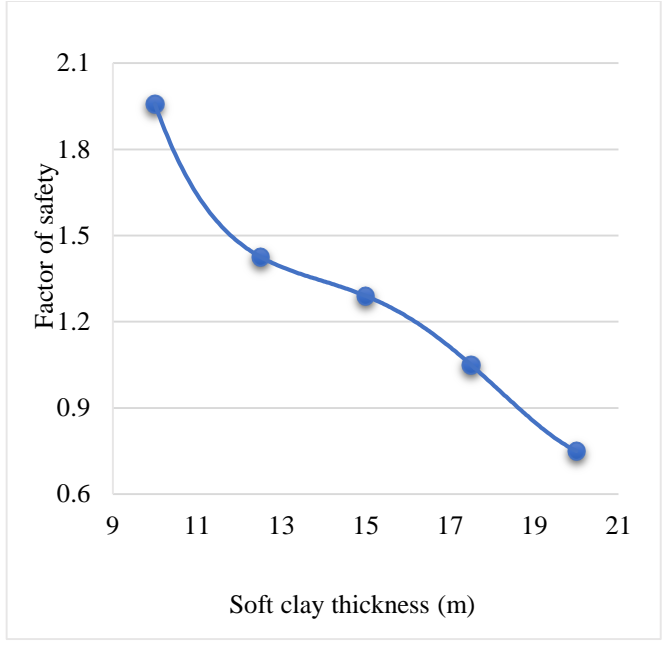


Fig. 29 Factor of safety changes with the thickness of the soft clay layer.

Figure 29 shows that the factor of safety drops as the soft clay layer gets thicker. Thicker clay layers lower the slope's shear resistance and create more potential surfaces for failure, especially under uniform loading. As a result, slope stability becomes more critical when the soft clay is deep.

3.2.7. Effect of Crushed Stone Replacement with Soft Clay Soil

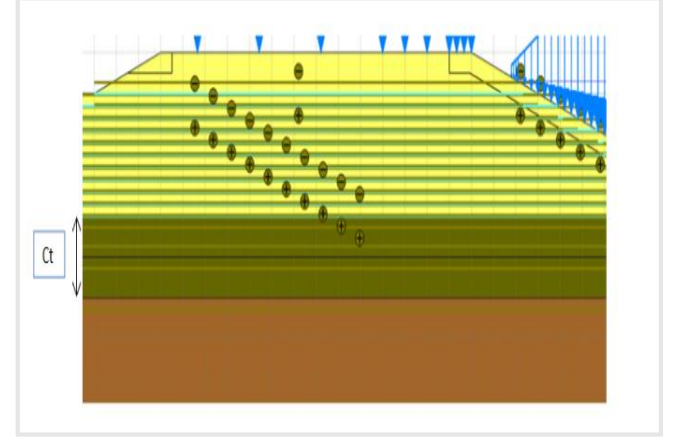


Fig. 30 Embankment with a crushed stone layer at the foundation

Figure 30 shows the embankment setup with a crushed stone (Ct) layer at the foundation. To study how the thickness of the crushed stone affects embankment behavior, finite element analyses were performed for layers ranging from 0.25 m to 2.5 m under a uniform load of 33 kN/m.

The resulting vertical displacement, horizontal displacement, and factor of safety are presented in Figures 31 to 33.

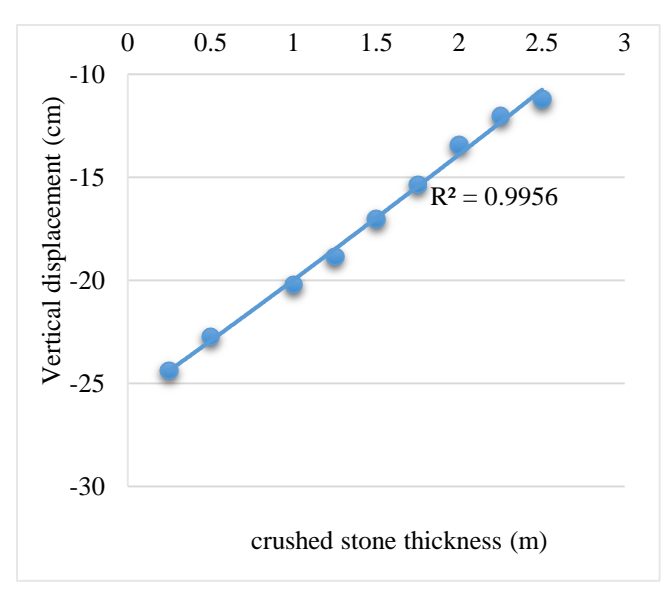


Fig. 31 Vertical displacement for different crushed stone thicknesses

Figure 31 shows that vertical displacement decreases as the crushed stone layer becomes thicker. The reduction continues up to a thickness of 2.5 m, after which there is little change. For layers thinner than 1 m, the vertical movement stays almost the same. Increasing the crushed stone thickness from 0.25 m to 2.5 m results in about a 53.9% decrease in vertical displacement.

Accordingly, the vertical displacement was estimated as a function of the crushed stone thicknesses using the empirical relationships given in Equation (21):

$$VD = 0.1627(T)^{2} + 5.7095(T)$$

$$-25.815 (P < 0.001)$$
 (21)

Where:

VD = Vertical displacement (cm), T= crushed stone thickness (m)

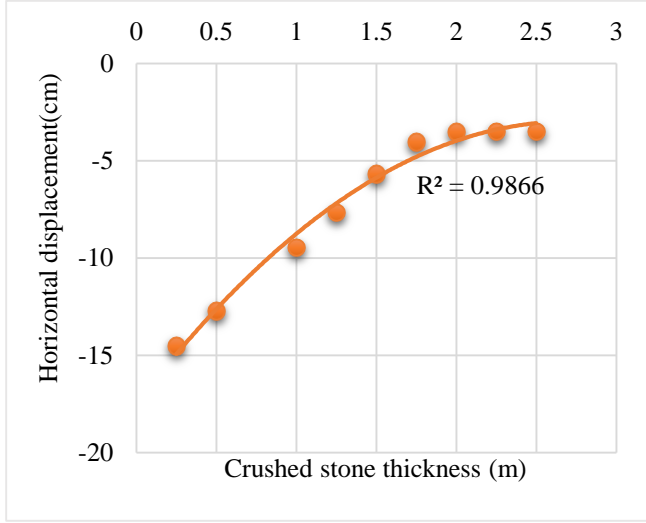


Fig. 32 Horizontal displacement for different crushed stone thicknesses

Figure 32 shows that horizontal displacement decreases as the crushed stone layer becomes thicker. The reduction continues up to a thickness of 2.5 m, after which little change occurs. For layers thinner than 1 m, the horizontal movement stays almost the same. Increasing the crushed stone thickness from 0.25 m to 2.5 m results in about a 75.9% decrease in lateral displacement.

Accordingly, the vertical displacement was estimated as a function of the crushed stone thicknesses using the empirical relationships given in Equation (22):

$$HD = -1.9763(T)^2 + 10.705(T) - 17.48$$

$$(P < 0.001) \tag{22}$$

Where:

HD = Horizontal displacement (cm), T= crushed stone thickness (m)

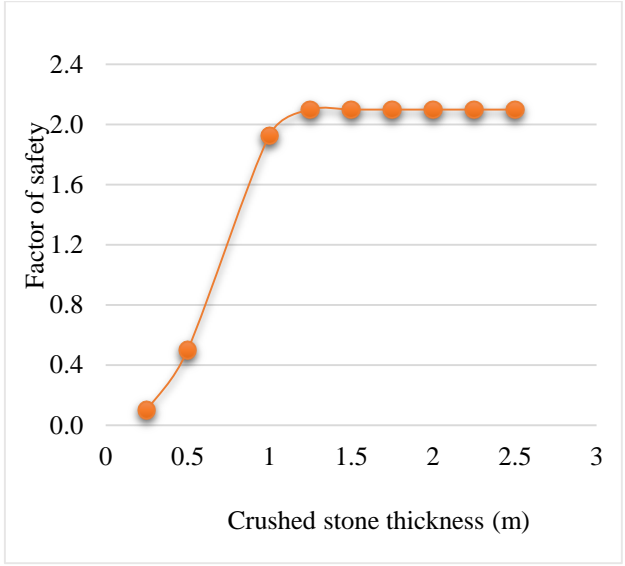


Fig. 33 Factor of safety for different crushed stone thicknesses

Figure 33 shows that the factor of safety rises as the crushed stone layer becomes thicker. A thicker layer helps strengthen the base, making the slope more stable and reducing possible deformation in the underlying soft clay.

4. Conclusion

We studied how geogrid-reinforced embankments with a crushed stone layer perform in stabilizing canal sections. A Finite Element Model (FEM) was used, and it was checked against field data. The model predicted vertical and horizontal displacements very close to what was observed in the field, with about 97% and 94% match. These results show that the model matches how the slope actually behaves. We can use it to come up with simple empirical equations. The parametric study highlighted how changes in soil properties and reinforcement parameters influence the stability of the embankment.

- Axial Stiffness: When the geogrid stiffness was increased, both vertical and horizontal displacements got smaller. This effect continued up to a point that depended on the load applied. For 33, 60, and 90 kN/m, the best stiffness ranges were 5000–6500, 7500–10000, and 12000–15000 kN/m, respectively. We noticed that vertical movements decreased by 19.4%, 28.3%, and 37.9%. Horizontal movements also fell by 56.8%, 64.5%, and 67.8%. The slope's safety factor got better when the geogrid was stiffer.
- For Geogrid Spacing: layers that were farther apart caused the slope to move more vertically and horizontally. The safety factor decreased. Vertical displacement increased by 2.9%, 6%, and 24.5%, and horizontal displacement increased by 19.6%, 22.5%, and 36.2% for loads of 33, 60, and 90 kN/m.
- Soil Cohesion: Stronger clay improved the slope performance. Vertical displacement dropped by 19.9%, horizontal by 42.3%, and the safety factor improved when cohesion increased from 10 to 40 kPa.
- Modulus of Elasticity: Stiffer soil layers reduced movement. Vertical displacement decreased by 77.1% and horizontal by 83.8% for modulus values up to 8000 kPa. Beyond this, changes were small, but the slope was still more stable.
- Unit Weight: Heavier soil reduced both vertical and horizontal displacements. Vertical settlement dropped by 55.3% and horizontal by 74.1%. Safety improved.

- Clay Thickness: Thicker clay caused larger deformations.
 The vertical displacement went up by 75.6% and the horizontal displacement increased by 57.8%. At the same time, the slope became less safe.
- Crushed Stone Layer Thickness: Thicker crushed stone layers lowered displacements and improved the slope. Increasing the layer from 0.25 m to 2.5 m reduced vertical displacement by 53.9% and horizontal displacement by 75.9%. Layers thinner than 1 m had little effect. Improvements above 2.5 m were minor; the results were used to develop simple equations for estimating vertical and horizontal displacements in geogrid-reinforced soft clay. The equations were derived from numerical models that were checked against field measurements. They can help engineers plan and improve canal embankments in a more practical way. We can use these equations to reduce the number of geogrid layers. The crushed stone base can also be made thinner. This does not affect the slope's stability or performance. In future work, we should watch how the embankment behaves over a long time. We need to check things like creep and consolidation. Different geogrid materials and installation methods should also be tested.

Acknowledgments

All authors' names who participate in the manuscript are mentioned.

References

- [1] Braja M. Das, Cavit Atalar, and Eun Chul Shin, "Behaviour of Embankment over Soft Clay Supported by Geogrid and Concrete Piles," *Proceedings of the 11th International Conference on Geosynthetics*, Seoul, Korea, pp. 1-8, 2018. [Google Scholar] [Publisher Link]
- [2] Hany A. Lotfi, Mahmoud Y. Shokry, and Rami M. El-Sherbiny, "Three Dimensional Finite Element Analysis of Geogrid Reinforced Piled Embankments on Soft Clay," *EuroGeo*, pp. 1507-1517, 2016. [Google Scholar] [Publisher Link]
- [3] Marcio de Souza Soares de Almeida et al., "Ground Improvement Techniques Applied to Very Soft Clays: State of Knowledge and Recent Advances," *Soils and Rocks*, vol. 46, no. 1, pp. 1-32, 2023. [CrossRef] [Google Scholar] [Publisher Link]
- [4] M. Mushaathoni, and S. Naidoo, "High-Strength Geogrids for Enhanced Ground Improvement: Design Considerations," *Proceedings of the Geosynthetics Conference for Young Professionals*, Irene Country Lodge, Irene, Centurion, pp. 1-6, 2024. [Google Scholar]
- [5] Geosynthetic Materials Association, Geosynthetic Materials Association, The Association, 2003. [Publisher Link]
- [6] Kavitha S. Nair, and B.L. Deepthy, "Improvement of Soft Subgrade Using Geogrid Reinforcement," *International Journal of Engineering Research & Technology*, vol. 5, no. 8, pp. 1-3, 2017. [Google Scholar] [Publisher Link]
- [7] Shams A. Mohammed, Sepanta Naimi, and Ahmed H. AbdulKareem, "The Effect of Geogrid reinforcement of Embankment Over Soft Foundation," *Periodicals of Engineering and Natural Sciences*, vol. 10, no. 6, pp. 5-27, 2022. [CrossRef] [Google Scholar] [Publisher Link]
- [8] Murad Abu-Farsakh, Qiming Chen, and Radhey Sharma, "An Experimental Evaluation of the Behavior of Footings on Geosynthetic-Reinforced Sand," *Soils and Foundations*, vol. 53, no. 2, pp. 335-348, 2013. [CrossRef] [Google Scholar] [Publisher Link]
- [9] Deepanshu Agrawal, and Mohit Verma, "Analysis of Geogrid Reinforced Road Embankment using PLAXIS 2D," *International Journal for Research Trends and Innovation*, vol. 6, no. 8, pp. 1-4, 2021. [Google Scholar] [Publisher Link]
- [10] Jorge G. Zornberg, and Edward Kavazanjian Jr, "Prediction of the Performance of a Geogrid-Reinforced Slope Founded on Solid Waste," *Soils and Foundations*, vol. 41, no. 6, pp. 1-16, 2001. [CrossRef] [Google Scholar] [Publisher Link]
- [11] E.M. Comodromos, M.C. Papadopoulou, and N.S. Klimis, "Design of Reinforced Embankments: Limit Equilibrium and Numerical Methods," 9th International Conference on Geosynthetics, Brazil, pp. 1835-1838, 2010. [Google Scholar]
- [12] B.R. Christopher, and L.G. Schwarz, "Performance of Geogrids Overlying Geotextiles in Roadway Stabilization Applications," 9th International Conference on Geosynthetics, Brazil, pp. 1451-1456, 2010. [Google Scholar] [Publisher Link]

- [13] Ahmet Demir et al., "Experimental and Numerical Analyses of Circular Footing on Geogrid-Reinforced Granular Fill Underlain by Soft Clay," *Acta Geotechnica*, vol. 9, pp. 711-723, 2014. [CrossRef] [Google Scholar] [Publisher Link]
- [14] Robert M. Koerner, Designing with Geosynthetics, 6th ed., Xlibris US, vol. 1, pp. 1-526, 2012. [Google Scholar] [Publisher Link]
- [15] ASTM D1557-12(2021), Standard Test Methods for Laboratory Compaction Characteristics of Soil Using Modified Effort (56,000 ft-lbf/ft3 (2,700 kN-m/m3)), ASTM International, pp. 1-13, 2021. [CrossRef] [Publisher Link]